

RESEARCH ARTICLE

Targets with cone-shaped microstructures from various materials for enhanced high-intensity laser–matter interaction

Tina Ebert¹, René Heber¹, Torsten Abel¹, Johannes Bieker², Gabriel Schaumann¹, and Markus Roth¹

¹Institut für Kernphysik, Department of Physics, Technische Universität Darmstadt, 64289 Darmstadt, Germany

²Integrierte Mikro-Nano-Systeme, Department of Electrical Engineering and Information Technology, Technische Universität Darmstadt, 64283 Darmstadt, Germany

(Received 1 December 2020; revised 21 January 2021; accepted 26 February 2021)

Abstract

Targets with microstructured front surfaces have shown great potential in improving high-intensity laser–matter interaction. We present cone-shaped microstructures made out of silicon and titanium created by ultrashort laser pulse processing with different characteristics. In addition, we illustrate a process chain based on moulding to recreate the laser-processed samples out of polydimethylsiloxane, polystyrol and copper. With all described methods, samples of large sizes can be manufactured, therefore allowing time-efficient, cost-reduced and reliable ways to fabricate large quantities of identical targets.

Keywords: microstructured targets; moulding; particle acceleration; ultrashort laser pulse processing; X-ray generation

1. Introduction

Recent studies have shown that targets with nanostructured and microstructured front surfaces are capable of enhancing the output of high-intensity laser-based X-ray and particle sources^[1–4]. This is mostly attributed to the highly light-absorbing properties of these structures, as well as a change in terms of electron heating mechanisms. By transferring more energy from the laser into the target the conversion efficiency is improved, which is especially important for smaller laser systems. In particular, newly developed laser systems are capable of repetition rates of several kilohertz^[5], and along with this advancement the demand for large quantities of identical targets increases^[6]. Therefore, it is of great interest that target manufacturing procedures are time- and cost-efficient while also guaranteeing high quality and reproducibility.

Depending on the application, different microstructure geometries and materials are required. There are several methods available for fabrication including etching, two-photon polymerisation, laser processing, pulsed laser depo-

sition and various moulding techniques^[7,8]. Recently, cone-shaped microstructures have attracted the interest of the community^[9,10]. Her *et al.*^[11] discovered the formation of such conical needles on silicon wafer surfaces after exposing them to a series of ultrashort laser pulses. The interference of the incident and scattered light creates a spatial variation in the intensity, and laser-induced periodic surface structures (LIPSS) with a distance of the order of the laser wavelength develop. Self-focusing of the subsequent pulses deepens these so-called ripples, eventually resulting in cone-shaped microstructures. Further studies have shown that the size and form of these structures can be adjusted without much effort by changing the laser and processing parameters^[12–15]. This technique is well studied for silicon, but also works with other materials such as titanium or aluminium^[16]. It can be applied to large areas and is rather cost-efficient, making ultrashort laser pulse treatment a reliable tool for target fabrication.

To further expand the amount of available materials, the laser structured samples can be used as the master in a subsequent moulding process. For high-precision moulding, polydimethylsiloxane (PDMS) was observed to feature excellent properties with regards to resolution and handling^[17,18]. This polymer can be used to cast an impression of the master,

Correspondence to: T. Ebert, Schlossgartenstr. 9, 64289 Darmstadt, Germany. Email: tebert@ikp.tu-darmstadt.de

resulting in a mould with inverse geometry. The mould is then employed to manufacture the original microstructure from a different material. This versatile process chain further optimizes the overall fabrication effort.

This paper describes experimental procedures to fabricate silicon, titanium, PDMS, polystyrol (PS) and copper microstructures as well as layered targets based on structured silicon wafers. Subsequently, the advantages and future steps are discussed.

2. Method

Depending on the desired target material, different approaches to manufacture microstructured targets are chosen. Laser-induced structuring is applied to Si and Ti whereas replication based on moulding processes yields PS and Cu microstructures. In addition, fabrication procedures for layered targets consisting of Si microstructures and a PS or Cu rear layer are described.

All samples are characterised with a scanning electron microscope (SEM) with an additional conductive coating if necessary. The high-aspect structures have proven to be challenging for atomic force microscopy and their highly light-absorbing properties make characterisation with optical microscopy difficult. Cross sections of the Si targets can be viewed after snapping the structured wafers. By aid of pre-cut lines, either by a diamond cutter or a short-pulse laser, the position of the break is predetermined.

2.1. Ultrashort laser pulse processing

The experimental setup to fabricate the laser-induced microstructures is based on an ultrashort-pulse Ti:sapphire laser system. It consists of an oscillator with a central wavelength of 800 nm and a bandwidth of more than 40 nm as well as a successive amplifier, which delivers 200 μ J pulses at 5 kHz. The pulse duration is set to 100 fs. The average power at the process chamber can be adjusted continuously between 50 and 800 mW with the aid of a polariser and an adjustable waveplate. Before entering the processing chamber, the beam passes a focusing lens. The position of the lens can be adjusted to precisely align the focal plane relative to the substrate. Then, the beam is reflected by a set of two galvanometric mirrors, which allow the laser to be moved rapidly across the substrate surface. The substrate is scanned with an approximately 70 μ m focus (full width at half maximum (FWHM)), therefore allowing the fabrication of microstructured areas of various sizes. Scanning the sample multiple times results in a homogeneously structured area. Because laser-induced surface structuring is a material-removing process, the overall thickness of the wafer is successively reduced with each scan.

The installed processing chamber can be used to create a vacuum or be filled with different gases. It is optimised to minimise the chamber volume to reduce the amount of processing gas needed while also keeping the distance between substrate and laser entry window large enough to prevent damage to the glass from the converging laser. A description of process chambers for our particular laser setup suitable for air or liquid processing media can be found in Ref. [15].

Figure 1(a) shows a cross section of a Si substrate processed in a 600 mbar SF₆ environment. The combination of ablation, slight melting and etching results in sharp needle-like structures. Their size depends both on the energy and the number of laser pulses hitting the same spot. For this sample, the averaged power was kept constant at 150 mW but the number of pulses was increased from 250 to 1250 toward the right, therefore gradually increasing the height of the structures. It is crucial to choose the right distance between the scanned lines, in this case 25 μ m, to obtain an overall homogeneously structured area. With the described method, any desired combination of structure height, base thickness and frame thickness can be dialled in. Depending on the specific parameter combination, the thickness of the initial substrate varies.

For some laser-matter experiments it might be interesting to orient the microstructures in or against the direction of the incident high-intensity laser. By tilting the substrate during the structuring process slanted needles can be produced as shown in Figure 1(b). As the structures always point in the direction of the incoming processing laser, the tilt is directly linked to the slant angle.

To create microstructured targets with a particular geometry an empirical dial-in procedure is applied to find the correct parameter set. This starts with choosing the processing medium and the incidence angle, which determines the shape and the slant angle, respectively. Then, the optimal distance between the scanned lines is determined by structuring a small area (e.g. 500 μ m \times 500 μ m) in the respective processing medium with different distances. The velocity, which is typically between 0.5 and 5 mm s⁻¹, and the fluence are fixed and should not be changed afterwards. In particular, the latter influences the width of the structured line, because relevant permanent changes to the surface arise only if the fluence exceeds the ablation threshold. These thresholds depend on the material, the processing medium and the laser parameters. For silicon in SF₆ with our laser parameters the ablation threshold is approximately 2 kJ m⁻²[12]. Afterwards, the samples are checked with an optical microscope to find the scanning distance that yields the most homogeneous area. This parameter is then used during the subsequent scans. To determine the total number of pulses necessary, several areas are scanned with varying numbers of repeats. By breaking the samples, their cross section can be evaluated with an SEM to measure the height of the structures and the remaining base thickness. If the values do not match

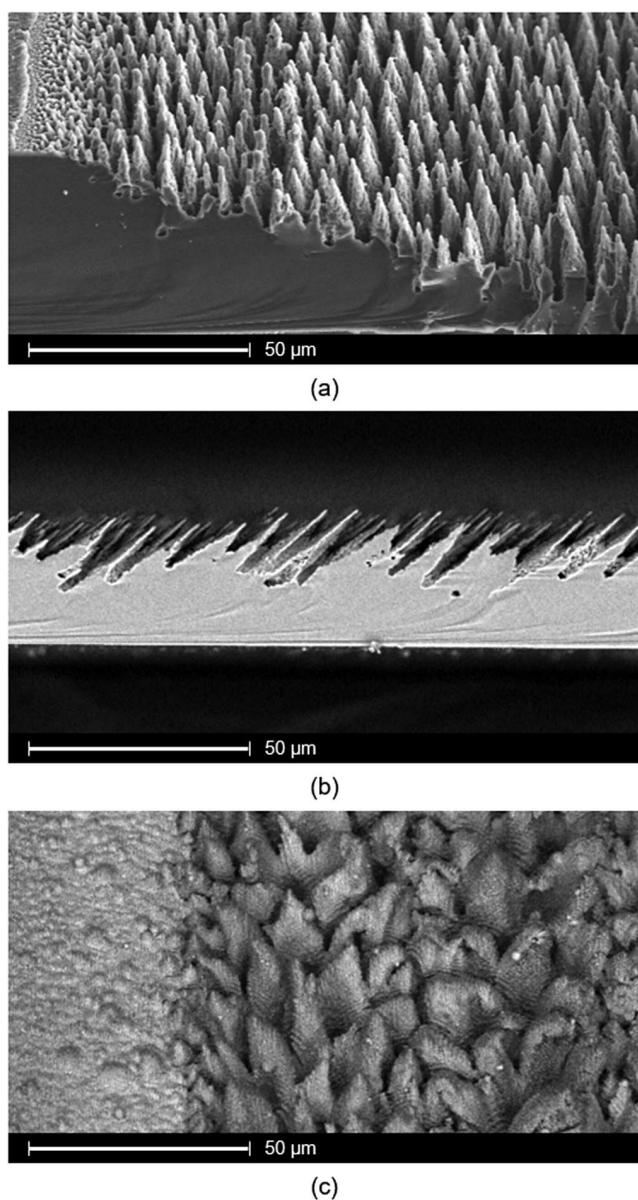


Figure 1. SEM images of laser-induced microstructures. The top and middle images show cross sections of Si processed in 600 mbar SF_6 . For (a) the pulse number was increased from 0 to 1500 pulses from left to right at a fluence of approximately 8 kJ m^{-2} . The sample is viewed at 30° . The slanted structures in (b) are created with a laser incidence angle of 45° , a fluence of approximately 9 kJ m^{-2} and roughly 1000 pulses. This sample is viewed at 90° . The bottom image (c) shows Ti microstructures fabricated in 7 mbar vacuum with different laser fluences. Low fluences below the ablation threshold lead to ripples (left third) whereas higher fluences (up to 20 kJ m^{-2}) generate broad cones (two thirds on the right).

the desired design, a substrate with a different thickness is chosen or the number of scans is adjusted.

With the described setup, both Si and other solid-state substrates can be structured. The right-hand side of Figure 1(c) shows a Ti sample processed in a vacuum with a residual air pressure of 5 mbar with 110 pulses at 500 mW. The resulting microstructures are broader and more irregular,

and also show a different substructure on the cone surfaces compared with Si needles.

2.2. Replication

In case the desired material cannot be structured by ultra-short laser pulse processing, a replication process based on a moulding procedure can be employed. Here, casting is used to fabricate similar cone-shaped microstructures from other materials. The process is illustrated in Figure 2. First, a master is produced, e.g., by ultrashort laser pulse processing, and placed in a container. In this case, microstructured Si samples are employed as masters. Then, an anti-sticking coating is applied to ease the peeling off of the mould. For this, the sample is placed in a desiccator together with a small amount of chlorotrimethylsilane. Under low pressure the silane evaporates and coats the master.

For the moulding of microstructures, the material used needs to have excellent resolution properties. One substance frequently used in other areas such as nanofluidics and microfluidics is PDMS^[19], which is comparatively inexpensive, straightforward to handle and can be removed without difficulty from the master because it is flexible once solidified. The PDMS Sylgard 184 by DowCorning^[20] is mixed with a 10:1 ratio of base and cross-linker as recommended by the manufacturer. Degassing the polymer after stirring as well as placing the master, on which the PDMS is poured, in a desiccator removes trapped air bubbles, therefore leading to a precise impression of the original sample. The polymer is degassed for 60 min at room temperature and then cured at 100°C for another 30 min to accelerate the solidification process. Figure 3 shows a silicon master and its mould with the clearly visible substructures on both samples.

After carefully peeling the mould of the master it is used in two different ways. One option is the replication with a polymer such as PS, which can be either deuterated or non-deuterated as both solutions can be handled in the same way. For this replication, the mould is placed in a spin coater with a toluene atmosphere, which prevents the PS solution ($0.104 \text{ g PS per } 1 \text{ mL toluene}$) from irregularly solidifying. Then, a drop of the solution is applied with a syringe before spinning the sample at 3000 r/min for 60 s. The result is a thin, approximately $15 \mu\text{m}$ thick, microstructured foil that can be placed on a target frame.

The second possibility is replication via electroplating with, e.g., Cu. As this method requires a conducting seed layer on the surface of the PDMS mould, which is a dielectric, the cold sample is coated by thermal evaporation with 10 nm Cr and a 90 nm thick seed layer of Cu. The Cr is necessary to improve the bonding between polymer and metal. Next, the mould is placed in an electrolytic cell filled with Tifoo Bright Copper Plating Solution^[21]. It is coated for 60 min at room temperature with a current density of

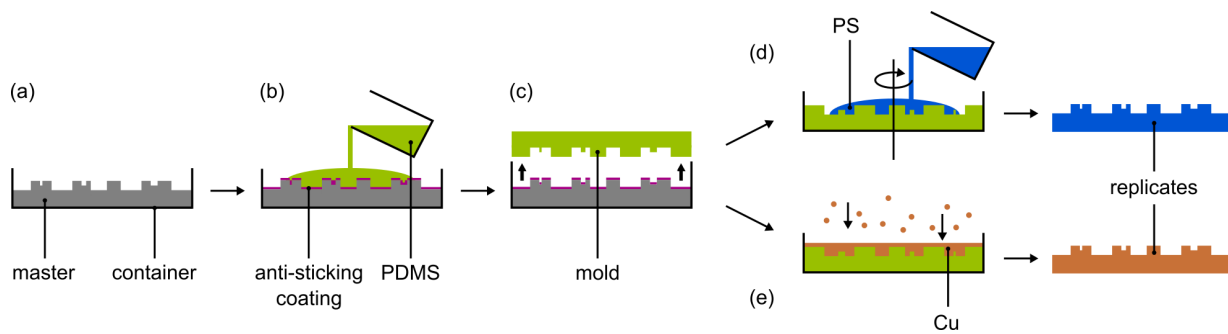


Figure 2. Replication procedure. (a) The Si master is placed in a container and coated with an anti-sticking coating before (b) PDMS is poured onto it. (c) After solidification, the PDMS is removed and can then be used as a mould to either create (d) a PS replicate by spin coating or (e) a Cu replicate by thermal evaporation followed by electroplating.

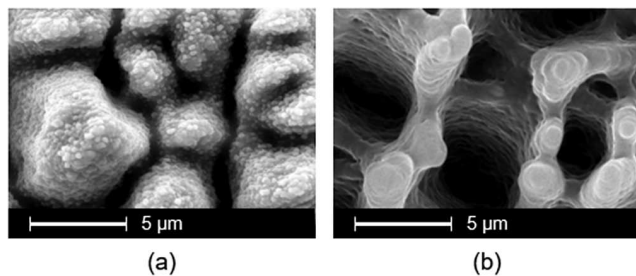


Figure 3. SEM images in top view of (a) Si needles fabricated in a SF₆ environment and (b) a different section of the respective PDMS mould. The nanometre substructures of the master are clearly visible in the mould.

approximately 6 A dm^{-2} . During the deposition, an agitator keeps the electrolyte in motion to prevent the creation of inhomogeneities in the Cu layer, e.g. by H₂ production or local depletion of the electrolyte. Afterwards, the sample is thoroughly cleaned with distilled water to remove any excess electrolyte. Lastly, the approximately 25 μm thick microstructured Cu foil is carefully removed with a scalpel.

As the Cu is deposited on an uneven surface, the rear side of the resulting foil can exhibit protruding features. Their size depends on the dimensions of the microstructures in the mould and on the final thickness of the foil, as this unevenness is smoothed out during the deposition process. For thin targets requiring a flat rear surface it therefore might be necessary to add a subsequent polishing or grinding step.

Figure 4 shows a Si master and PS and Cu replicates. Although the sub-micrometre structures slightly differ due to shrinking or swelling, the overall shape is very similar, which shows the remarkable replication capabilities of this process chain.

2.3. Layered targets

For some experiments it is not strictly necessary that the whole target is made of the same material. Previous studies showed the great potential of layered target designs with flat front surfaces^[22,23]. Combining specific microstructures

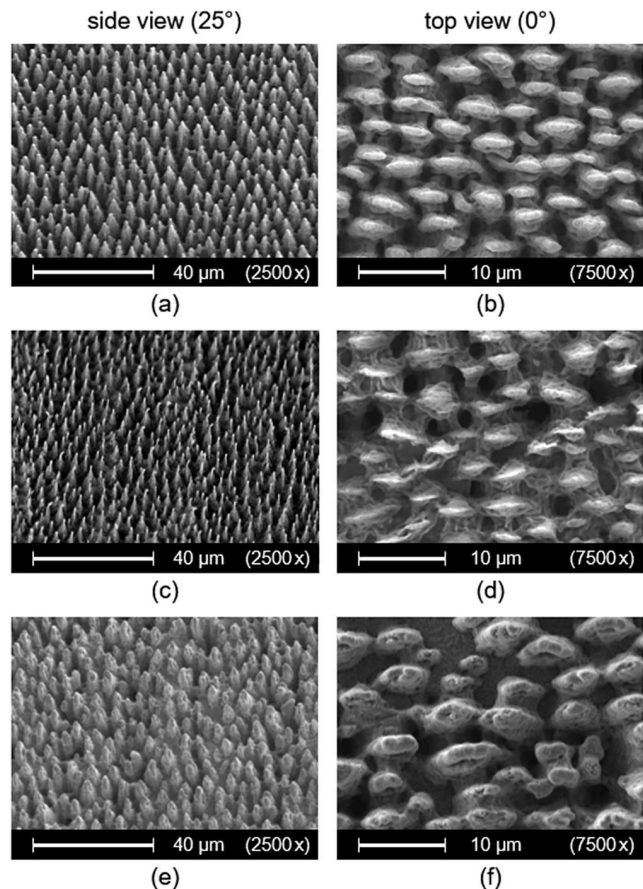


Figure 4. SEM images viewed from the side with an approximate angle of 25° (left column) and from the top (right column). The top row shows a Si master, the middle row a PS replicate and the bottom row a Cu replicate. The lower magnification (2500×) of the side view illustrates the distribution and cone-shape of the structures whereas the higher magnification (7500×) of the images in top view shows the sub-micrometre features as well as the diameter of the structures.

with favoured materials is expected to further enhance the particle and radiation output for secondary applications. As the structuring process is well known for Si and allows for a wide variety of structure shapes and sizes, this material is used as the target front component.

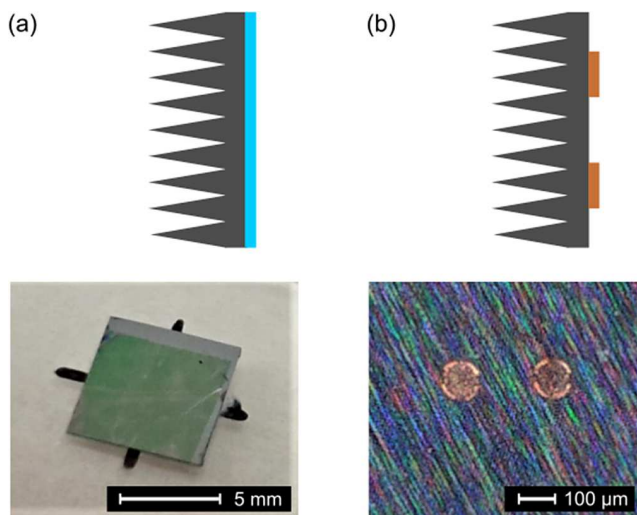


Figure 5. Layered target configurations as schematic (top row) and photo (bottom row). The PS foil (a) appears greenish on the rear side of the Si wafer with front surface microstructures. To create a defined laser-driven X-ray source, Cu microdots (b) are applied to the Si wafer before structuring the opposite side.

In particular, for laser ion acceleration and neutron generation a proton- or deuteron-rich layer at the target rear side is of great interest. For this, thin polymer foils are produced via spin coating^[24] on a glass wafer, which are then detached by submerging the wafer into distilled water so that the foils float on the surface. With the structured Si targets already mounted on a target frame, the foils are carefully lifted out of the water. Given the correct angle and speed, the foils cling to the Si wafer without any additional adhesive. An exemplary target is shown in Figure 5(a).

Targets used for X-ray generation often require a high-Z material. In this case, sputtering, electroplating or thermal evaporation can be employed to add the required layer. By using masks, the layer does not have to coat the entire target, but can also be restricted to specific areas. Figure 5(b) shows an image of a Cu microdot target. Here, the Cu dots are manufactured by thermal evaporation in combination with a 25 μm Ni mask. Afterwards, the front side of the respective Si wafer is structured with ultrashort laser pulses.

3. Discussion

Experiments studying different aspects of laser–matter interaction are numerous and require a wide range of target materials. In particular, the reproduction process can be easily transferred to manufacture cone-shaped microstructures from, e.g., silver, nickel and gold electrolytes or nanopowder and polymer mixtures to meet the experimental requirements.

In addition, the moulding procedure reduces the expenditure of time and costs as one mould can be re-used multiple

times. Obviously, the described process chain is applicable to all sorts of microstructures and macrostructures.

Another advantage of the PDMS moulds described here is that they are flexible and can therefore be shaped into different macroscopic geometries before continuing the replication process.

Furthermore, all described methods facilitate the fabrication of very large structured areas, which in our case is mainly restricted by the respective containers and processing chambers. For usage in further experiments, the samples are laser cut to fit the specific target setups. In this way, by creating large samples a large number of targets with identical properties can be produced for, e.g., high-repetition-rate experiments.

The presented procedures allow the customisation and optimisation of the target design for respective experimental campaigns. To find the optimal geometry for a specific laser configuration, parameter scans can be performed by fabricating microstructures with varying geometries and dimensions, which is within reasonable effort as most of the processing parameters can be easily modified. Previous studies^[10,25] discussed that the influence of the microstructures on the energy transfer between laser and target not only depends on the properties of the target, such as the material, cone geometry and distribution, but also on the laser parameters, among which pulse length and contrast are key factors. Depending on the amount of energy deposited before the main pulse, the microstructures will retain their overall geometry or dissolve. This, in turn, influences the electron heating mechanisms involved in the energy transfer between laser and target, which are a variable composition of Brunel heating on the intact, sloped structure sides and resonant absorption in the valleys filled with preplasma.

4. Summary

In summary, fabrication procedures for cone-shaped microstructures from various materials for enhanced laser–matter coupling have been presented. Whereas silicon and titanium can be structured directly via ultrashort laser pulse processing, microstructured surfaces on PS and copper substrates can be manufactured by moulding with PDMS. The moulding process chain enables the replication of the exact same structure geometry. In addition, methods for building layered targets have been presented. This variety of materials meets the requirements of a wide field of laser–matter interaction experiments, which can all benefit from the excellent absorption properties of the discussed microstructures.

Acknowledgements

The authors would like to thank Steffen Sander of the Target Laboratory of the Institute of Nuclear Physics, as well as

Sebastian Dehe of the Institute for Nano- and Microfluidics and the team of the Integrated Micro- and Nanosystems Laboratory at the Technical University of Darmstadt for their support during the development of the fabrication processes. This project received financial support from the DFG in the framework of the Excellence Initiative, Darmstadt Graduate School of Excellence Energy Science and Engineering (GSC 1070), the BMBF (05P19RDF A1) and the Hessian Ministry for Science and the Arts (HMWK) through the LOEWE Research Cluster Nuclear Photonics at TU Darmstadt.

References

1. S. Jiang, A. G. Krygier, D. W. Schumacher, K. U. Akli, and R. R. Freeman, *Phys. Rev. E* **89**, 013106 (2014).
2. O. Klimo, J. Psikal, J. Limpouch, J. Proska, F. Novotny, T. Ceccotti, V. Floquet, and S. Kawata, *New J. Phys.* **13**, 053028 (2011).
3. D. A. Serebryakov, T. M. Volkova, E. N. Nerush, and I. Y. Kostyukov, *Plasma Phys. Control. Fusion* **61**, 074007 (2019).
4. M. Passoni, A. Sgattoni, I. Prencipe, L. Fedeli, D. Dellasega, L. Cialfi, I. W. Choi, I. J. Kim, K. A. Janulewicz, H. W. Lee, J. H. Sung, S. K. Lee, and C. H. Nam, *Phys. Rev. Accel. Beams* **19**, 061301 (2016).
5. C. N. Danson, C. Haefner, J. Bromage, T. Butcher, J.-C. F. Chanteloup, E. A. Chowdhury, A. Galvanauskas, L. A. Gizzi, J. Hein, D. I. Hillier, N. W. Hopps, Y. Kato, E. A. Khazanov, R. Kodama, G. Korn, R. Li, Y. Li, J. Limpert, J. Ma, C. H. Nam, D. Neely, D. Papadopoulos, R.R. Penman, L. Qian, J. J. Rocca, A. A. Shaykin, C. W. Siders, C. Spindloe, S. Szatmári, R. M. G. M. Trines, J. Zhu, P. Zhu, and J. D. Zuegel, *High Power Laser Sci. Eng.* **7**, e54 (2019).
6. I. Prencipe, J. Fuchs, S. Pascarelli, D. W. Schumacher, R. B. Stephens, N. B. Alexander, R. Briggs, M. Büscher, M. O. Cernaianu, A. Choukourov, M. De Marco, A. Erbe, J. Fassbender, G. Fiquet, P. Fitzsimmons, C. Gheorghiu, J. Hund, L. G. Huang, M. Harmand, N. J. Hartley, A. Irman, T. Kluge, Z. Konopkova, S. Kraft, D. Kraus, V. Leca, D. Margarone, J. Metzkes, K. Nagai, W. Nazarov, P. Lutoslawski, D. Papp, M. Passoni, A. Pelka, J. P. Perin, J. Schulz, M. Smid, C. Spindloe, S. Steinke, R. Torchio, C. Vass, T. Wiste, R. Zaffino, K. Zeil, T. Tschentscher, U. Schramm, and T. E. Cowan, *High Power Laser Sci. Eng.* **5**, e17 (2017).
7. X. Liu, P. R. Coxon, M. Peters, B. Hoex, J. M. Cole, and D. J. Fray, *Energy Environ. Sci.* **7**, 3223 (2014).
8. P. van Assenbergh, E. Meinders, J. Geraedts, and D. Dodou, *Small* **14**, 1703401 (2018).
9. M. Blanco, M. T. Flores-Arias, and M. Vranic, *arXiv:1902.05641* (2019).
10. T. Ebert, N. W. Neumann, L. N. K. Döhl, J. Jarrett, C. Baird, R. Heathcote, M. Hesse, A. Hughes, P. McKenna, D. Neely, D. Rusby, G. Schaumann, C. Spindloe, A. Tebartz, N. Woolsey, and M. Roth, *Phys. Plasmas* **27**, 043106 (2020).
11. T.-H. Her, R. J. Finlay, C. Wu, S. Deliwala, and E. Mazur, *Appl. Phys. Lett.* **73**, 1673 (1998).
12. T.-H. Her, R. J. Finlay, C. Wu, and E. Mazur, *Appl. Phys. A* **70**, 383 (2000).
13. B. K. Nayak and M. C. Gupta, *Opt. Lasers Eng.* **48**, 966 (2010).
14. Y. Peng, X. Chen, Y. Zhou, K. Luo, and Y. Zhu, *Appl. Phys. B* **118**, 327 (2015).
15. T. Ebert, N. W. Neumann, T. Abel, G. Schaumann, and M. Roth, *High Power Laser Sci. Eng.* **5**, e13 (2017).
16. B. K. Nayak and M. C. Gupta, *Opt. Lasers Eng.* **48**, 940 (2010).
17. P. O. Caffrey, B. K. Nayak, and M. C. Gupta, *Appl. Opt.* **51**, 604 (2012).
18. F. Hua, Y. Sun, A. Gaur, M. A. Meitl, L. Bilhaut, L. Rotkina, J. Wang, P. Geil, M. Shim, J. A. Rogers, and A. Shim, *Nano Lett.* **4**, 2467 (2004).
19. J. Friend and L. Yeo, *Biomicrofluidics* **4**, 026502 (2010).
20. <https://www.dow.com/en-us/pdp/sylgard-184-silicone-elastomer-kit.01064291z.html> (October 14, 2020).
21. <https://www.tifoo.de/en-uk/acidic-bright-copper-plating-solution> (October 13, 2020).
22. J. Badziak, E. Woryna, P. Parys, K. Y. Platonov, S. Jabłoński, L. Ryć, A. B. Vankov, and J. Wołowski, *Phys. Rev. Lett.* **87**, 215001 (2001).
23. H. Schwoerer, S. Pfothner, O. Jäckel, K.-U. Amthor, B. Liesfeld, W. Ziegler, R. Sauerbrey, K. W. D. Ledingham, and T. Esirkepov, *Nature* **439**, 445 (2006).
24. A. Tebartz, S. Bedacht, G. Schaumann, and M. Roth, *J. Phys. Conf. Ser.* **713**, 012005 (2016).
25. M. Blanco, M. T. Flores-Arias, C. Ruiz, and M. Vranic, *New J. Phys.* **19**, 033004 (2017).